HORIBA Scientific

Fluorescence

Monitoring Biotinylated Adeno-Associated Virus (AAV) Complexed to Streptavidin-Alexa Fluor 568 using the Aqualog and A-TEEM Molecular Fingerprinting Method

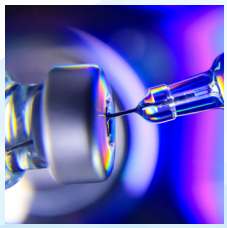

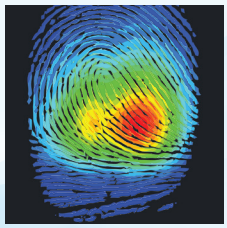

Application Note
Life Sciences
FL-2021-07-22

Introduction

Adeno-Associated Viruses (AAVs) are becoming widely used as viral vectors to deliver cell and gene therapies and vaccines. As production methods scale to meet growing demand, more information is needed more quickly. The transition of these technologies from R&D into the biopharmaceutical mainstream has applied pressure on analytical technologies to keep pace. In this note we explore the use of HORIBA's fluorescence A-TEEM™ (Absorbance-Transmittance Excitation Emission Matrix) technology to rapidly (<90 sec) differentiate biotinylated AAV samples that are complexed with streptavidin-dye conjugates from uncomplexed AAVs. We believe it is possible to develop quantitative models to test the efficiency of complexation, although this will be the subject of future work to prove.

One key advantage of AAVs is that different serotypes target specific cell-types, delivering therapies directly to their intended target. Modifying AAVs to extend their affinity for specific cell types is the subject of R&D efforts, and requires tools to determine the efficiency of targeting for these modified vectors. [ref 2] One method to monitor AAV transduction targeting and efficiency starts with biotinylated AAV particles. Biotin has a very strong affinity for streptavidin and offers a well-known approach for staining and targeting of biomolecules, allowing targeting specificity and efficiency to be characterized.

A-TEEM is a rapid (seconds to minutes of data collection) optical technique combining UV/VIS/NIR absorbance with three dimensional fluorescence spectroscopy. It is fully validatable using NIST-traceable standards following USP chapters <853> and <857>. We report the ability of A-TEEM spectroscopy combined with multivariate analysis methods to: 1) differentiate biotinylated AAVs from AAV-dye complexes, with the potential for quantitative modeling; 2) distinguish biotinylated AAVs from streptavidin-dye conjugates (SAF568); and 3) quantify the removal of free dye and unbound streptavidin from the AAV Complex solution during dialysis. We discuss how A-TEEM spectroscopy and multivariate analysis could be of significant interest to AAV technology researchers and manufacturers for assessing their AAV applications including process efficiency for QA/QC purposes.

Materials and Methods

Samples and Preparation

The following samples were used in these experiments:

A. AAV: Biotinylated recombinant AAV
B. SAF568 Conjugate: Alexa Fluor 568 labelled streptavidin
C. AAV-SAF568 Complex: Fully linked AAV-Streptavidin Alexa Fluor 568
D. SAF568 Conjugate – dialyzed
E. AAV-SAF568 - dialyzed

Suspensions were diluted to reach Beer-Lambert linearity for A-TEEM analysis using PBS buffer. Figure 1 shows schematics of how these components were combined to make the conjugate and complex, as well as the result of the dialysis step for samples D) and E).

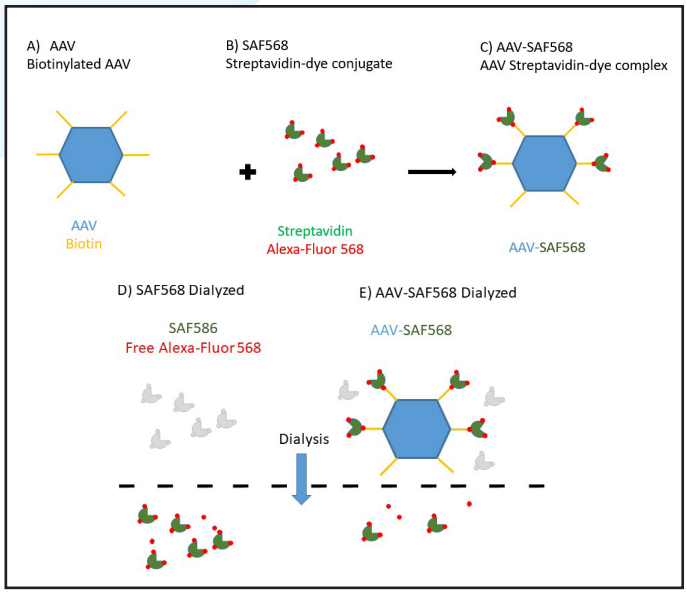

Figure 1: Presents schematic representations of the samples studied. 1A) Shows an AAV capsid with biotin functionalization. Biotin binds strongly with streptavidin, providing a mechanism to label compounds with fluorescence dyes. 1B) Is the streptavidin-dye conjugate (SAF568) where Alexa Fluor 568 is conjugated to the protein. 1C) shows the entire complex (AAV-SAF568), where dye bound to streptavidin is complexed to the AAV using the biotin functional groups. Dialysis was used to remove unbound protein-dye conjugate and free dye from the Conjugate and Complex samples. Figure 1D and 1E illustrate the relative permeabilties of the free dye (red circles) and SAF568 protein conjugate relative to the AAV-SAF568 complex. The dialysis membrane and relative permeability pore size are represented by the dashed line, and the direction of dialysis is denoted by the downward arrow.

A-TEEM Measurements

All A-TEEM measurements were made with a HORIBA Aqualog UV-800C (Piscataway, NJ) using Aqualog software (v4.2). Samples were equilibrated to and maintained at 6° C and stirred in the sample chamber. The excitation and absorbance range was 240-700 nm at 5 nm increments and emission range was 250-800 nm at 4.66 nm and interpolated to 5 nm increments. The CCD was binned by 8 pixels and the Gain was medium with 1 s integration. All instrumental and sample bias corrections were applied including dark offset removal, blank solvent subtraction, NIST-traceable excitation and emission spectral correction, inner filter effect correction and water Raman scattering unit normalization. Integration time resulted in <90 s per A-TEEM acquisition.

Multivariate Analyses

All multivariate analyses were performed using Eigenvector Inc. Solo (v8.8). A-TEEM data preprocessing for Alexa Fluor 568 region Parallel Factor Analysis (PARAFAC) included the following steps: nonnegative constraints for scores and loadings and masking of the first and second order Rayleigh and Raman lines (16 and 32 nm, respectively). PARAFAC for the UV-autofluorescence region additionally included normalization. A-TEEM data block pre-processing for Principal Components Analysis (PCA) and Hierarchical Cluster Analysis (HCA) included: unfolding the 3-way matrix into a 2-way array, normalization and class-dependent automatic clutter removal, centering and scaling.

Results

A-TEEM Contour Analysis of AAV, SAF568, and AAV-SAF568 Samples

Table 1 gives literature fluorescence excitation and emission maxima for some of the expected components in these samples.

Tryptophan - protein bound	λ Max Excitation (nm)	λ Max Emission (nm)	Reference
Buried (non-polar)	280	330-332	Groza
Limited water exposure		340-342	
Water Exposed		350-353	
Tyrosine	274	303	
Phenylalanine	257	280	
Alexa Fluor 586	578	603	Thermo
Streptavidin	295		
native	295	335	Jurzban
denatured	295	348	

Table 1

Figure 2 shows the A-TEEM contours of the samples: 2A) AAVs - biotinylated; 2B) SAF568 - streptavidin with Alexa Fluor 568 dye conjugate; 2C) AAV-SAF568 complex; 2D) SAF568 after dialysis; and 2E) AAV-SAF568 complex after dialysis. Each A-TEEM is scaled to its peak contour intensity, so intensity between A-TEEMs are not comparable.

Table 2 summarizes the excitation and emission maxima for the A-TEEMs in Figure 2. The biotinylated AAV sample (2A) shows strong UV autofluorescence ex/em (280/330 nm), which is predominately due to buried tryptophan, i.e. in a non-polar environment. The SAF568 conjugate (which includes free dye in the undialyzed sample 2B) has strong fluorescence signal at ex/em (578/610) and ex/em (275/608 nm), as would be expected from the fluorescence dye used for labeling. This conjugate sample also has an autoflourescence feature at ex/em (278/332 nm) which is characteristic of natively folded streptavidin [ref 3].

	λ Max Excitation (nm)	λ Max Emission (nm)	Assignment
AAV	280	330	buried trp
Alexa Fluor 568	578	610	dye
Dye - UV	275	608	dye - UV response
SAF568 undialzyed	278	338	streptavidin
SAF568 dialyzed	270	303	tyr - low snr
AAV Complex undialyzed	278	332	buried trp
AAV Complex dialyzed	278	333	buried trp
PC 1 - AAV	280	325	buried trp
PC 2 - Streptavidin		335	streptavidin

Table 2

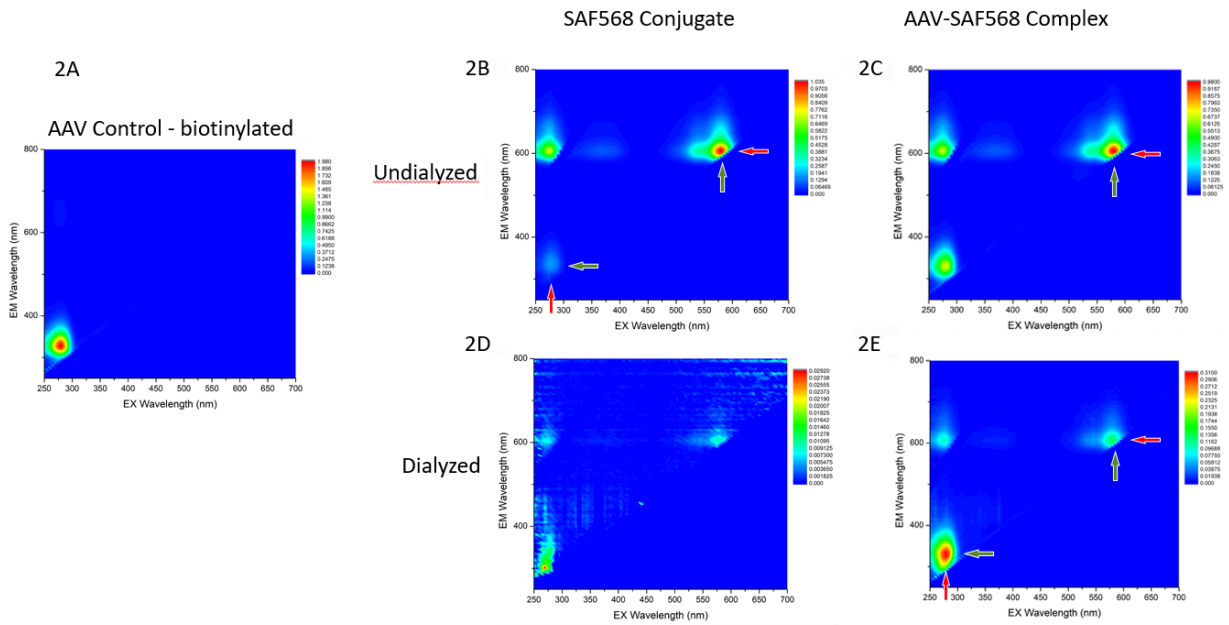

Figure 2: A-TEEM contours for 2A) biotinylated AAV; 2B) SAF568 dye-protein conjugate; 2C) AAV-SAF568 complex; and dialyzed versions of 2D) SAF568 conjugate and 2E) AAV-SAF568 complex. Contours are uniquely scaled to the maximum peak intensity of that EEM, so comparisons of intensities between EEMs is not possible. The green (excitation) and red (emission) arrows in A point to the main peak attributed to Alexa Fluor 568. The purple (excitation) and blue (emission) arrows in B point to the peak of the UV autofluorescence signal.

The dialysis process seems to remove both dye and the streptavidin-dye complex (2D), and the fluorescent signal is reduced by two orders of magnitude. The EEM of the AAV-streptavidin-dye complex in 2C has features of both the AAV and streptavidin-dye conjugate, unsurprisingly. Upon dialysis of the complex (2E), the UV autofluorescence from protein-bound aromatic amino acids predominates, with the fluorescent dye signals substantially reduced.

Discussion

Differentiate AAV Controls from AAV-SAF568 Complex with Autofluorescence, no Dialysis.

There is no "cross-talk" between the dye-induced visible fluorescence and UV autofluorescence signals from the tyrosine and tryptophan residues, so we truncated the data to exclude the visible dye portion of the EEM, focusing only on autofluorescence in the UV region, using emission from 250 - 500 nm and excitation from 250 - 400 nm. We used several multivariate methods to explore these signals, with the goal to decompose the autofluorescence spectra into separate and chemically meaningful signals that would aid in classifying the different materials.

The first approach was Parallel Factor Analysis (PARAFAC), which is a tri-linear principal components analysis yielding orthogonally correlated excitation and emission spectral loadings and scores for a designated number of components to describe samples in the data set. The analysis was performed using undialyzed samples only, comprised of 12 samples each of the AAV and SAF568 conjugate samples, and 16 samples of the AAV-SAF568 complex. Two components adequately accounted for the variance. The goodness of fit was summarized as accounting for 98.14% of the variance captures with a split-half validation matching percentage of 99.1%, which confirms that the user-selected model parameters have been appropriately selected.

Figures 3A and 3B show the differences between the excitation-emission loading contours for each component, while Figure 3C highlights the emission spectral loadings to illustrate the main spectral difference between the 2 components. Component 1 exhibited a peak wavelength of 325 nm compared to 335 nm for Component 2. From the values reported in table 1, and a peak at 335 nm we anticipate that Component 2 will describe streptavidin in its natively folded state.

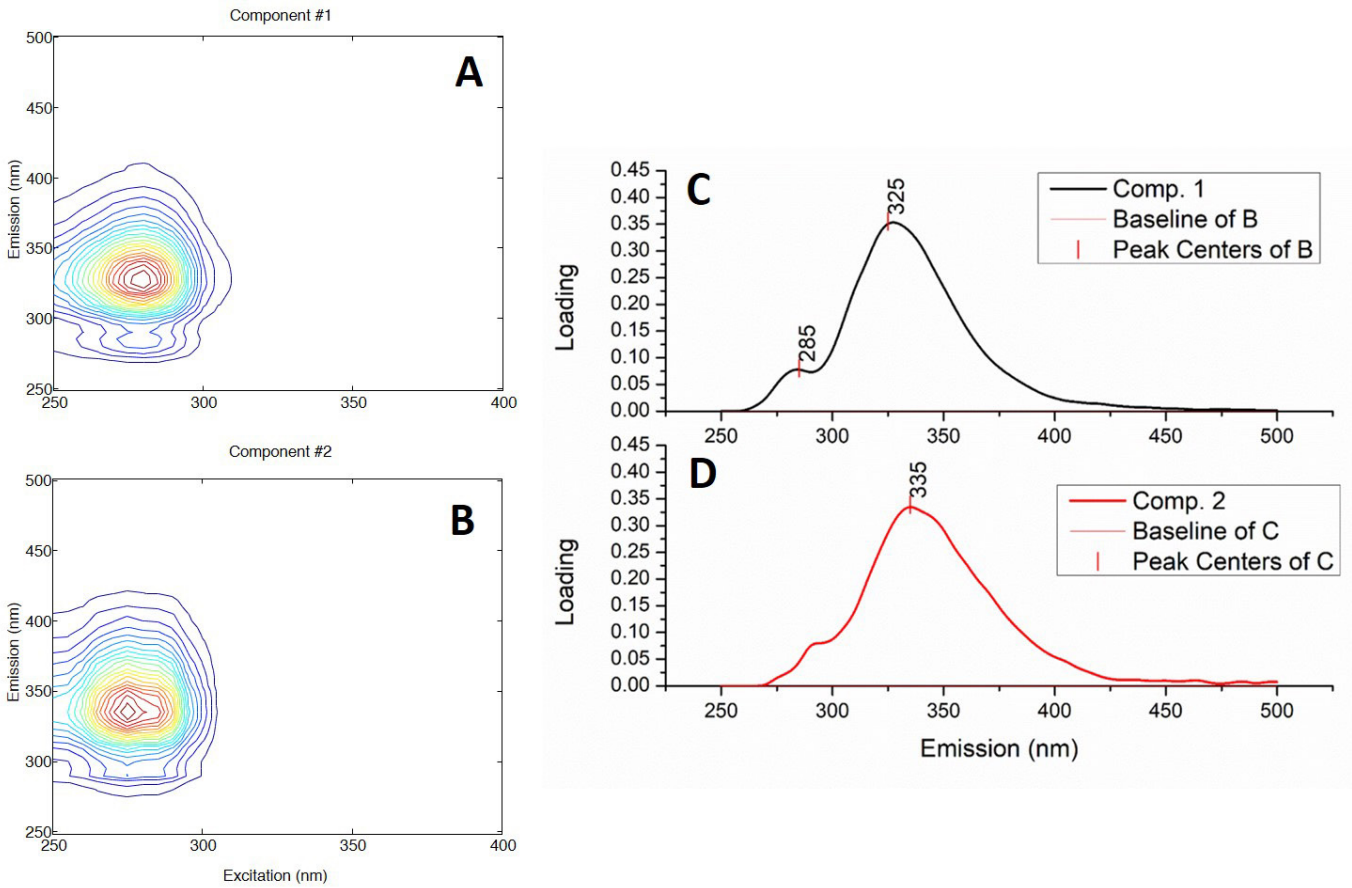

Figure 3: The excitation-emission loading contour plots for PARAFAC components 1 (A) and 2 (B) for the exclusive UV autofluorescence signal region for the AAV-SAF568, SAF568 and AAV control samples. Panels C and D compare the emission spectral loadings for the same PARAFAC model to show the differences in the peak center values. The component 2 emission spectral loading resembles the fluorescence emission spectrum for streptavidin in its native-folded state.

To check the validity of this, Figure 4 shows the PARAFAC scores for Component 1 plotted against Component 2 where the three sample types AAV, AAV-SAF568 and SAF568 are represented by green, blue and red symbols respectively; the confidence ellipses represent a 95 % confidence level.

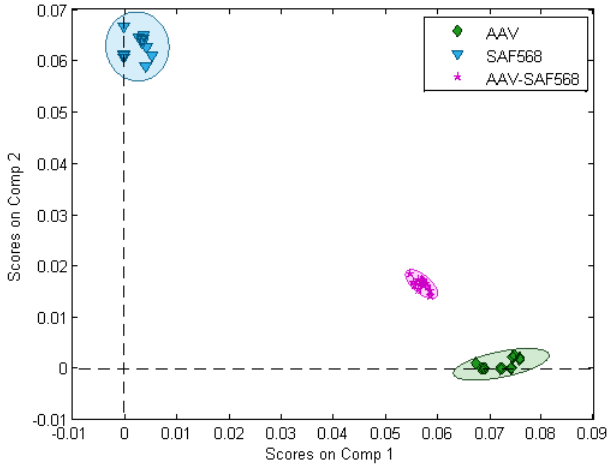

Figure 4: Evaluation of the PARAFAC score clusters for components 1 (abscissa) and 2 (ordinate) for the class groups defined in the legend as AAV-SAF568, SAF568 and AAV. The confidence level for the ellipses was 95%. The AAV-SAF568 complex samples have contribution from both Component 1 (AAV) and Component 2 (streptavidin), although more closely resemble the AAV.

Component 2 does indeed describe the SAF568 contour, while Component 1 describes biotinylated AAV. The AAV-SAF568 complex exhibits a mixture of the two components, but has significantly higher levels of Component 1 (AAV) than 2 (streptavidin). This analysis shows that AAV-dye complexes can be differentiated from unbound AAVs using the UV autofluorescence of undialyzed samples. It is likely that a quantitative model built on a titration of samples of known concentrations could be used to quantify complexation in unknowns. Due to the lack of standardized samples of known concentration, this is beyond the scope of this note.

Further Multivariate Explorations to Differentiate AAV Controls from AAV-SAF568 Complex

The relationships among the samples was further evaluated using the more standard Principal Components Analysis (PCA) where the 3-way EEM data is first unfolded into a 2-way array. Preprocessing also included normalization, Class Centroid Centering and Scaling and clutter removal using a General Least Squares weighting of 0.02. It is notable that PARAFAC does not support centering, scaling or clutter removal, so in some cases PCA can provide higher confidence levels and precision for purposes of discrimination. The PC 1 and PC 2 both accounted for 100% of the variance at 96.55 and 3.45%, respectively. Figure 5 shows that each of the sample types exists in a unique quadrant for the plot of PC 1 and PC 2; the data classes are each defined with a 99% confidence ellipse that is actually much smaller than the symbol size as scaled. Thus consistent with the data above, it is clear that PCA also has the ability to discriminate the AAV, SAF568 and AAV-SAF568 complex samples.

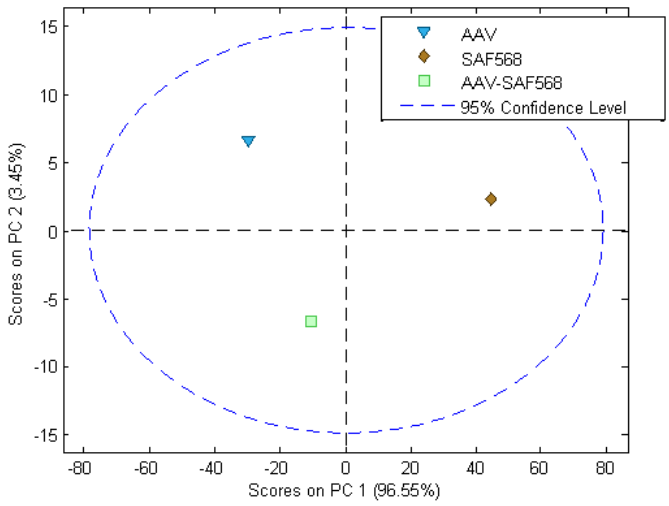

Figure 5: Evaluation of the PCA score clusters for components 1 (abscissa and 2 (ordinate) for the class groups defined in the legend as AAV-SAF568, SAF568 and AAV. The confidence level for the ellipses was 95%, although the ellipses are not visible, being smaller than the symbol size. This shows very strong classification between these three samples.

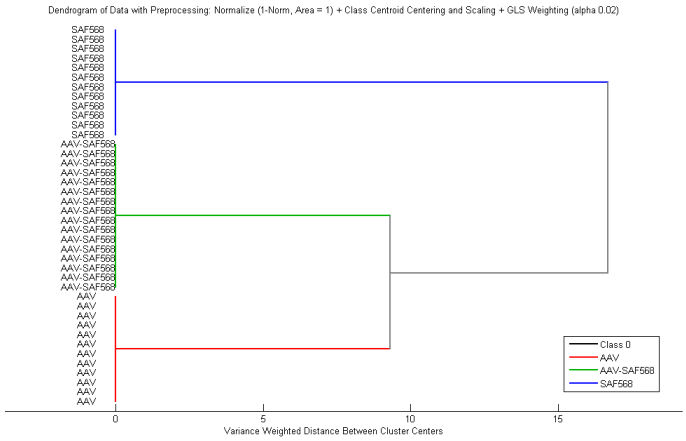

Figure 6. Evaluation of the HCA cluster dendrogram for the class groups defined in the legend as AAV-SAF568, SAF568 and AAV. The analysis, based on the PCA results, shows definitive separation between the samples. These results agree with the PARAFAC analysis, in which the AAV-SAF568 was seen to be more closely related to the AAV than the protein-dye conjugate.

Effect of Dialysis on AAV-SAF568 Complex and SAF568 Conjugate

Figures 2B and 2D highlight the effects of dialysis on SAF568, the streptavidin-dye conjugate, with each A-TEEM scaled to its own peak contour intensity. Both A-TEEMs exhibit three major ex/em contours, one attributed to Alexa Fluor dye fluorescence [ex/em (579/610 nm & 275/608 nm), and the other to autofluorescence of the streptavidin protein, ex/em (278/338 nm). Dialysis strongly diminished all fluorescence signals, suggesting the treatment removed a large fraction of both the streptavidin protein, free dye, and protein-dye conjugate. Figures 2C and 2E show the effects of dialysis on the AAV-SAF568 complex, with each A-TEEM scaled to its own peak contour intensity.

As seen with SAF568, the A-TEEMs exhibit three major fluorescence excitation/emission (ex/em) contours; one attributed to the Alexa Fluor 568 dye with a peak at [ex/em (578/610 nm & 275/608 nm) and the other to autofluorescence of the AAV tryptophan residues at ex/em (280/330 nm). The ratio of the red Alexa Fluor peak to the autofluorescence peak was clearly diminished from 1.43 before dialysis to 0.43 after, indicating the treatment preferentially removed the SAF568 protein-dye conjugate and free dye in solution.

Figure 7A plots the before (black) and after (red) dialysis intensities of the Alexa Fluor dye fluorescence component signal from AAV-SAF568 complex as a function of dilution with PBS. Both the before and after series showed strong linear correlations over the observed dilution range; the slope for the before and after samples was 377.293 and 16.0597, respectively. Figure 7B shows the linear fits for the SAF568 protein-dye conjugate samples before and after dialysis also exhibit strong linear correlations; the slope for the before and after samples was 666.8293 and 2.59206, respectively. Figure 4C compares the before:after slope ratios for the AAV-SAF568 complex and SAF568 conjugate samples from Figures 7A and 7B to indicate that dialysis diminished both slopes to a large extent, with a significantly larger (close to a factor of 7) effect on the SAF568 conjugate. This analysis, along with the A-TEEM contour analysis in Figure 2, suggests the dialysis is preferentially removing unbound SAF568 protein-dye conjugate and free Alexa Fluor 568 dye compared to the AAV-SAF568 complex.

Conclusion

A quick look at the A-TEEM contours in Figure 2A-2C supports the idea that the A-TEEM method may be sensitive to differences between biotinylated AAV capsids and AAVs complexed with a protein-dye conjugate. However, the presence of the Alexa Fluor 568 dye might be expected to obscure native fluorescence that could be useful in quantifying these samples. We show in this note that it is possible to differentiate biotinylated AAVs from AAV-dye complexes for undialyzed samples, with significant free dye and protein-dye conjugate present. The PARAFAC analysis separates the signal for the complex into two main components which seem to be attributable to AAV and streptavidin. With standard reference samples of each of these, we anticipate that A-TEEM could be used to create a quantitative model against which unknown samples could be quantified for complexation efficiency. PCA was used to easily distinguish AAVs from protein-dye conjugates, and from AAV-protein-dye complexes. We were also able to quantify the removal of free dye and unbound streptavidin from the AAV Complex solution during dialysis.

Thus we conclude that the Aqualog and A-TEEM, when coupled with standard multivariate analysis techniques such as PARAFAC, PCA and HCA, can be used to effectively monitor binding and purification of AAV materials important to research and industrial applications.

References:

1. “Metabolic Biotinylation Provides a Unique Platform for the Purification and Targeting of Multiple AAV Vector Serotypes”, G. S. Arnold, et al., Molecular Therapy 14, 1, 2006, pp 97-106.
2. “Site Specific Modification of AAV Enables Both Fluorescent Imaging of Viral Particles and Characterization of the Capsid Interactome”, J. S. Chandran et al., Scientific Reports 7:14766, 2017, pp 1-17.
3. “The Quarternary Structure of Streptavidin in Urea”, G. P. Kurzban, et al., Journal of Biological Chemistry 266, 22, 1991, 14470-14477.
4. “Anisotropy Resolved Multi-dimensional Emission Spectroscopy (ARMES): a New Tool for the Quantitative and Structural Analysis of Proteins”, R. C. Groza, thesis submitted NUI Galway, 2016

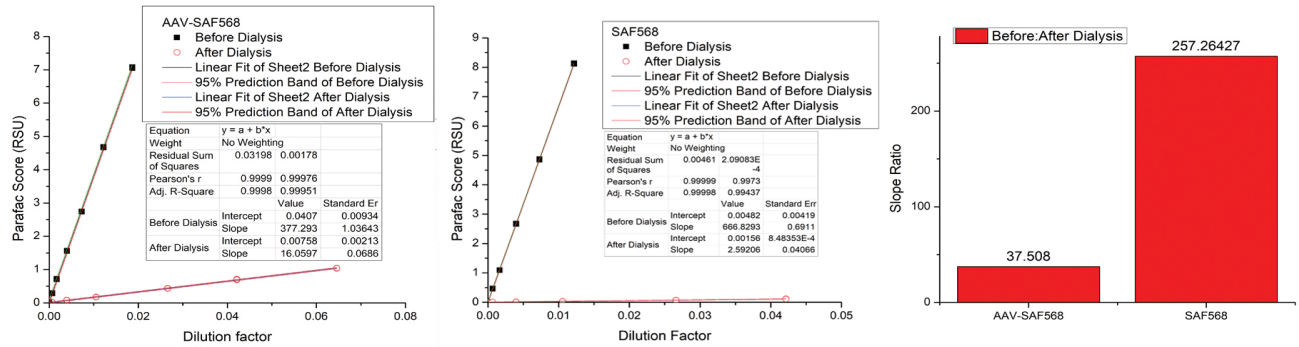

Figure 7: Linear regression analyses of the Alexa Fluor 568 component scores for the AAV-SAF568 (A) and SAF568 (B) samples before (black) and after (red) dialysis as a function of dilution of the stock with PBS buffer. Panel C compares the ratios of the slopes Before:After dialysis for the samples in A and B. The legends provide details on the linear fit and prediction band lines, as well as the linear regression statistics.

To learn more about the A-TEEM technique and applications go to **A-TEEM.com**

JOBIN YVON Technology

info.sci@horiba.com **www.horiba.com/scientific**

HORIBA Scientific

USA: +1 732 494 8660
UK: +44 (0)1604 542 500
China: +86 (0)21 6289 6060
France: +33 (0)1 69 74 72 00
Italy: +39 06 51 59 22 1
Brazil: + 55 (0)11 2923 5400
Germany: +49 (0) 6251 8475 20
Japan: +81 (0)3 6206 4721
Other: +1 732 494 8660